Lasers in Surgery and Medicine 18:367–372 (1996)

Electron Paramagnetic Resonance Spectroscopy of Free Radicals in Corneal Tissue Following Excimer Laser Irradiation

G.H. Pettit, MD, PhD, M.N. Ediger, PhD, D.W. Hahn, PhD, R.J. Landry, MS, R.P. Weiblinger, MA, and K.M. Morehouse, PhD

Food & Drug Administration, Center for Devices & Radiological Health, Rockville, Maryland 20857 (G.H.P., M.N.E., D.W.H., R.J.L., R.P.W.); Food & Drug Administration, Center for Food Safety & Applied Nutrition, Washington, DC 20204 (K.M.M.)

Background and Objective: **Free radicals, detected previously in corneal tissue following 193 nm laser irradiation, may be important agents in the laser/tissue interaction. Electron paramagnetic resonance spectroscopy (EPR) has been used to examine such radical formation in detail.**
Study Design/Materials and Methods: **Bovine corneal strips were frozen in liquid nitrogen, irradiated with excimer laser pulses, and assayed by EPR. Exposure conditions were varied to study radical formation dependence on laser intensity and repetition. Results were measured against a quantifiable standard to calculate radical quantum yield.**
Results: **Either weak or intense laser fluences produced comparable tissue EPR signals. Radicals accumulated in frozen tissue for at least 10 initial ablation pulses. Radical quantum yield in cornea was 0.15%.**
Conclusion: **Corneal radical formation is largely a photochemical process driven by the 193 nm laser radiation. Reactive radical species are produced in substantial numbers and likely have a significant clinical role.** © 1996 Wiley-Liss, Inc.*

Key words: ablation, photochemistry, photorefractive keratectomy

INTRODUCTION

The argon fluoride (ArF) excimer laser is being extensively studied worldwide as a clinical tool for remodeling the optical surface of the eye. Such intense interest has arisen because nanosecond 193 nm pulses from ArF lasers vaporize cornea with submicron precision and minimal collateral damage [1]. In a recent study of this laser/tissue interaction [2], using electron paramagnetic resonance spectroscopy (EPR) and cryogenic experimental conditions, we have detected organic free radicals in cornea following the irradiation. This finding is significant for two reasons. First of all, highly absorbing organic radicals could cause the enhanced attenuation of 193 nm laser radiation during ablation [3] and the associated small etch depth per pulse in the tissue (compared to the 1/e laser penetration depth). Of greater practical importance, the ancillary tissue damage caused by such reactive species may contribute to the complex healing response that is observed clinically, that is, "haze" formation and curvature regression [4–6]. In support of this contention, a recent study involving rabbits has shown a significant postoperative haze reduction in animals treated with radical scavengers just before laser exposure [7].

Our initial EPR study was essentially qualitative in nature, documenting that organic radi-

Accepted for publication February 23, 1995.

Address reprint requests to George H. Pettit, M.D., Ph.D., F.D.A. Center for Devices & Radiological Health, Mail Stop HFZ-134, Rockville, MD 20857.

cals were formed in the cornea and were highly reactive (short lived) at physiologic temperatures. Radical EPR signatures were large, relative to noise, only for frozen corneal samples receiving multiple laser irradiations at each site on the de-epithelialized surface. This indicated that there was a net radical accumulation in the frozen tissue over multiple pulses, even though some absorbing fraction was etched away by each laser shot.

In this paper we pursue a more quantitative study of radical formation, taking the above-mentioned phenomena into account in determining a quantum yield of radicals produced per laser photon deposited. This is accomplished by measuring the tissue EPR signal amplitudes for varying delivered laser dosages, that is, different numbers of constant-fluence pulses per site, and by comparing these signals against that of a known radical-concentration standard. We also explore the photochemistry behind the radical formation by comparing tissue EPR signals for two distinct irradiation conditions involving the same delivered laser energy, one with a pulse fluence far below the ablation threshold and the other with a fluence well above threshold.

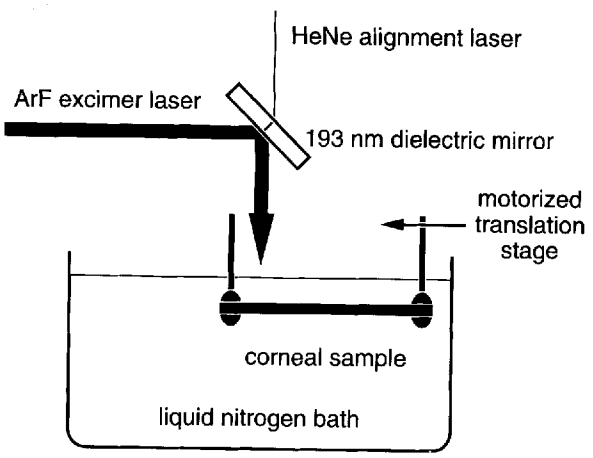

Fig. 1. Tissue irradiation apparatus. Corneal tissue samples were mounted in a horizontal brace and immersed in liquid nitrogen. The brace was fixed on a motorized translational stage so that the entire de-epithelialized sample surface could be exposed to a downward directed ArF laser beam in a controlled fashion. Cryogenic exposure conditions were necessitated by the radical reactivity at room temperature.

MATERIALS AND METHODS

Tissue samples used in this work were bovine corneas. Whole globes were obtained from a slaughterhouse and stored on ice until use less than 24 hours post mortem. Before laser irradiation, the central cornea of each globe was mechanically de-epithelialized and cut into rectangular strips measuring ~25 mm by 2 mm. Each strip was placed lengthwise on a glass stirring rod with the epithelial surface oriented upward and quickly immersed in liquid nitrogen (LN_2). This preserved the rectangular sample shape, and the slight curvature induced by the underlying rod helped identify the anterior sample surface.

The irradiation apparatus is shown in Figure 1. An ArF excimer laser beam was reflected by a dielectric mirror downward into an LN_2 bath containing the corneal tissue sample. A HeNe laser coaxial with the excimer beam was used for alignment. The sample was mounted on a horizontal brace just beneath the LN_2. The brace was fixed to a motorized translation stage that could pass up to 25 mm of the sample through the beam at a constant 0.5 mm/s. The laser spot size on the target was kept constant at 3.0 mm by 1.5 mm, with the shorter dimension oriented along the translation direction of the sample. Thus, the full sample width (2 mm) was exposed in the 3.0 mm wide beam as the tissue was translated lengthwise.

The ArF laser fluence per pulse was varied using a combination of lens, apertures, and neutral density filters. Two fluences were used in this study: 14 and 220 mJ/cm^2. These values were determined by measuring the pulse energy just after the dielectric mirror. (The liquid nitrogen reduced the laser fluence reaching the immersed tissue by an unknown amount, although a cursory examination suggested the radiation loss was small.) For reference, the ablation threshold fluence of bovine cornea, at room temperature, is ~30 mJ/cm^2 [8], and the fluences used in most human studies are in the 150–200 mJ/cm^2 range. Thus the lower experimental fluence used in this work was subablative, while the higher fluence approximated the clinical intensity and caused obvious etching of the frozen samples.

Following irradiation each sample was removed from the translation brace using stainless steel tweezers and held briefly beneath the surface of the LN_2 bath. A quartz EPR sample tube was immersed in the bath (filling it with LN_2), and the tissue strip was placed inside. The filled tube was then quickly transferred to a Dewar flask containing additional LN_2. While any particulate ablation debris would have remained in the bath, the possible contamination of the tube

by such debris was negligible. This was due to the fact that the bath volume (greater than 11) was much larger than the tube fluid volume assayed by EPR spectroscopy (~0.1 ml).

Measurements of radical formation were made using a Varian E-line Century Series EPR spectrometer. EPR spectroscopy works on the principle that paramagnetic species such as free radicals will absorb microwave radiation when placed in a strong magnetic field. The specific microwave frequency and field strength required depend on the nature of the absorbing radical species. In this study the microwave frequency was fixed at 9.19 GHz, and absorption was measured as the magnetic field was scanned over the range 2,880–3,280 G. The other relevant spectroscopy conditions were a magnetic field modulation amplitude of 5 G and a microwave power of 5 mW. Tissue samples were kept at LN_2 temperature throughout the EPR assay.

The initial experiment was a comparison of the radical generation efficiency by low and high fluence laser pulses. Twelve tissue samples were divided into two groups of six and irradiated with 900 mJ total laser energy (cumulative fluence ~2 J/cm^2). For the first group 14 mJ/cm^2 laser pulses were used, and the cumulative tissue dose was delivered by running the laser at 12 Hz and translating each sample 22.5 mm through the ArF laser beam four times. Each sample in the second group was irradiated with 220 mJ/cm^2 pulses at 3 Hz during a single 22.5 mm pass through the beam. EPR analysis was then performed on all samples under identical spectroscopic conditions, and the radical signatures for the two groups were compared.

The second experiment was a measure of radical accumulation in the frozen tissue under repetitive ablation conditions. With the laser running at 1/3 Hz, 15 220 mJ/cm^2 pulses were deposited at adjacent, essentially distinct, sites along 22.5 mm of a sample during one crossing through the beam. This corresponded to a dose of approximately 100 mJ. By increasing the laser repetition rate and/or the number of passes, higher laser dosages (200, 500, and 1,000 mJ) were delivered to subsequent samples, with repetitive trials conducted at each dose. Each sample was then assayed by EPR to determine relative amplitudes of the radical signals for the various laser dosages.

The third and final experiment was an absolute determination of radical yield under ablative conditions. A 1 J laser dose, which generated a pronounced EPR signal, was delivered to each of six tissue strips using ten 220 mJ/cm^2 pulses per site along a 22.5 mm length (150 pulses total). These samples were then assayed by EPR under the same spectroscopic conditions as those used to measure a 0.01 mM sample of diphenyl picryl hydrazyl (DPPH, a well-established EPR standard containing one radical per molecule). The EPR signals of the two materials were compared, and a quantum yield for laser radical formation in the tissue was calculated as described later.

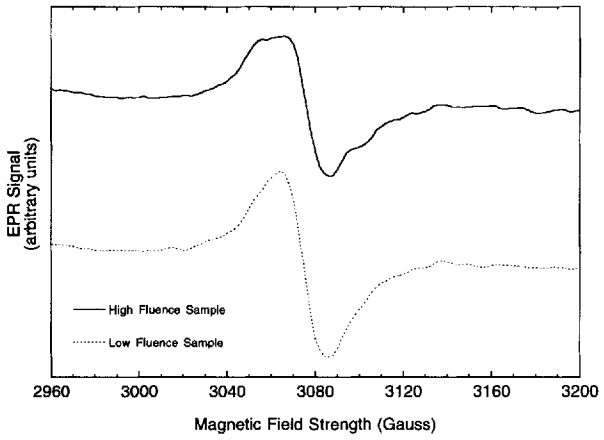

Fig. 2. Composite EPR spectra from corneal tissue samples irradiated with the same total laser energy (900 mJ), but using two distinct pulse fluences: 14 mJ/cm^2 (subablative) and 220 mJ/cm^2 (ablative). The two curves were obtained under identical spectroscopic conditions. Radical accumulation in the tissue, as determined by double-integration of the biphasic EPR signature, is roughly equivalent for the two laser intensity regimes.

RESULTS

Composite EPR tissue spectra from tissue samples irradiated at the two distinct pulse fluences are shown in Figure 2. The composite curves shown are the average of the six individual tissue spectra obtained at either fluence. Conventional EPR spectroscopy plots the *first derivative* of microwave absorption vs. magnetic field strength. Thus the single absorption "peak" characteristic of organic radicals appears as a biphasic feature in the derivative EPR trace.

The *absolute* number of radicals present in a sample is directly proportional to the second integral of the biphasic EPR spectrum. Double integration of the two spectra in Figure 2 produced values, in arbitrary units ±1 SD, of 90 ± 32 for the high-fluence spectra and 118 ± 27 for the low-fluence curves. Thus there was little statistical difference in radical accumulation for the two la-

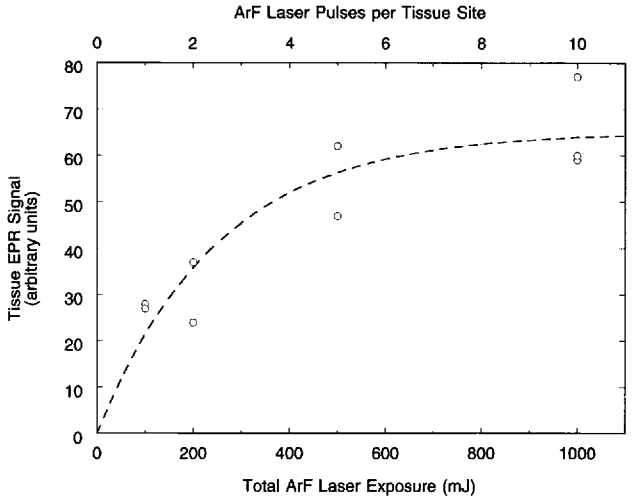

Fig. 3. EPR signal amplitudes from irradiated corneal tissue vs. ArF laser exposure. The laser fluence in each case was 220 mJ/cm^2 per pulse, which was clearly ablative. Each pass of the tissue through the beam deposited approxiamtely 100 mJ of laser energy onto a 2.25 × 0.2 cm area of the target. Radical accumulation clearly occurs over multiple exposures. The dashed curve is a simple model calculation described in the Discussion.

ser intensity regimes. The slightly different shapes of the two EPR profiles, for example, the distinct "shoulders" in the high intensity curve, suggest that the resultant radicals were chemically distinct for the two irradiation conditions.

The results of the repetitive irradiation study are shown in Figure 3. In determining the *relative* abundance of the same radical type in different samples, the peak-to-peak amplitude of the biphasic EPR signal can be used directly because the shape of the absorption feature is virtually the same for each specimen. In this particular experiment, the peak-to-peak signal amplitude was readily obtainable, even from the minimally irradiated samples, while double integration of the noisy weak spectra was not straightforward. The discrete points in Figure 3 indicate the peak-to-peak EPR signal amplitudes for samples irradiated with 1, 2, 5, or 10 ablative ArF laser pulses per site along the de-epithelialized tissue surface. Over these initial irradiations there was an accumulation of radical species in the frozen cornea, which neared a plateau by the 10th laser shot per site.

In the final experiment, the EPR spectrum from the 0.01 mM DPPH standard was much larger and narrower than those of the irradiated tissue samples. After the double integration was performed on all spectra, with differences in spectrometer gain taken into account, the radical content of the DPPH standard was calculated to be 2 × 10^4 larger than the average value for the corneal strips. The standard deviation in the tissue signal measurements was approximately 20%. Given that the DPPH contained ~6 × 10^{18} radical species, the implied average radical content for the corneal samples was 3 ± 0.6 × 10^{14}.

DISCUSSION

Free radicals can be formed in a variety of ways, including simple combustion reactions [9], as well as direct photochemical cleavage of absorbing molecules (e.g., ultraviolet "bond-breaking" of hydrogen peroxide into OH× [10]). The findings shown in Figure 2 indicate that ablative photodecomposition of cornea need not occur to form substantial radicals in the tissue target, since abundant radicals were produced at subablative laser intensity. Therefore photochemistry driven directly by the 193 nm laser radiation must be a major source of the tissue radicals. However, additional ablation-specific mechanisms for radical formation cannot be completely excluded by the two comparable EPR signal strengths of Figure 2. Radical accumulation during tissue ablation in LN_2 is obviously not a linear function of deposited laser pulses, as indicated in Figure 3, and the process may not be linear with repetitive irradiation at subablative fluences as well.

Since these species are highly reactive at physiologic temperatures, analogous radical accumulation over successive laser pulses does not occur in vivo. Nevertheless, the phenomenon shown in Figure 3 merits further consideration because it factors into the radical quantum yield calculation, which does have clinical relevance. In addition, analysis of the radical buildup in this experiment should be applicable to other irradiation products that are longer lived in the warm tissue.

The most likely reason for the nonlinear radical accumulation is that some radical species are lost from the corneal target with each ArF laser etching. This idea of competition between radical formation and ejection is the basis of the following model. In the corneal target, an incident 193 nm laser pulse of fluence F_0 is attenuated exponentially with depth x in the tissue as

$$F(x) = F_0 e^{-\alpha x}, \quad (1)$$

where α is the target absorption coefficient. It is assumed that the accumulation of free-radical absorbers in the solid is not enough to alter α significantly during repetitive irradiation. The laser energy absorbed at depth x in the cornea is noted as E(x), which is equal to $-dF/dx$. If q is the quantum yield of tissue radicals produced per laser photon absorbed, then C(x), the generated radical concentration vs. depth in the target, is given by

$$C(x) = \frac{qE(x)}{hv} = \frac{q\alpha F_0}{hv} e^{-\alpha x}, \quad (2)$$

where hv is the photon energy. The total radical content in the intact target after a single laser irradiation, R_1, can be found by integrating C(x) over all x. However, because of ablation the target surface is no longer at x = 0, but at the ablation depth, noted here as b. Thus

$$R_1 = A\int_b^\infty C(x)dx = \frac{AqF_0}{hv} e^{-\alpha b}, \quad (3)$$

where A is the irradiated target area. For a second irradiation an identical number of radicals will be *added* to the sample and must be summed with the residual fraction from the first pulse (i.e., that part not etched away by the second shot):

$$R_2 = R_1 + A\int_{2b}^\infty C(x)dx = \frac{AqF_0}{hv}(e^{-\alpha b} + e^{-2\alpha b}). \quad (4)$$

The cumulative radical yield after n irradiations will be

$$R_n = \frac{AqF_0}{hv}\sum_{k=1}^{n} e^{-k\alpha b}. \quad (5)$$

Equation (5) is almost directly applicable to the experimental data shown in Figure 3. The EPR peak-to-peak signal strength, S_n, should be equal to R_n times some constant experimental scaling factor (EPR counts per radical), noted here as s. By introducing two "lumped" constants,

$$a = \alpha b, \quad (6)$$

and

$$c = \frac{sAqF_0}{hv}, \quad (7)$$

the theory produces a simple equation to describe the measured results:

$$S_n = c\sum_{k=1}^{n} e^{-ka}. \quad (8)$$

The dashed curve in Figure 3 is the result of Equation (8) when the two equation constants are adjusted to provide a least-squares fit to the experimental data. Equation constants of a = 0.4 and c = 32 yield good agreement between the theoretical and measured values.

These constants have direct physical significance. Based on Equation (6) a value of 0.4 for a implies that the laser penetration depth ($1/\alpha$) is 2.5 times the ablation depth per pulse. For comparison, the reported small-signal penetration depth of 193 nm radiation in cornea is 3.7 μm [8], roughly *10* times larger than the ablation depths measured in numerous studies for ArF laser pulse fluences around 200 mJ/cm^2. This apparent discrepancy exists in part because the effective corneal penetration depth of ablative ArF laser pulses is markedly less than the small-signal value, as noted in the Introduction. Changes in corneal tissue properties upon LN_2 immersion may also contribute to the relatively small value for a.

The obtained value for c can be used in Equation (7) to calculate q, the radical quantum yield. All that is required is a value for s, the experimental scaling constant. The radical content of tissue samples ablated with 1 J total ArF laser energy is known from the third experiment to average 3×10^{14}. From Figure 3, a 1 J exposure produces a peak-to-peak EPR signal amplitude of ~64 units. Therefore s can be estimated to be 2.1×10^{-13} counts per radical. By using this along with the experimental values for the other variables in Equation (7), A = 0.45 cm^2, F_0 = 220 mJ/cm^2, and $h\nu = 1.0 \times 10^{-15}$ mJ, the quantum efficiency for radical generation is found to be 1.5×10^{-3}.

The one experimental finding not in good agreement with this simple theory is the roughly equivalent radical accumulation in the ablative vs. subablative irradiation (Fig. 2). According to the earlier analysis, the number of radicals per sample after the subablative irradiation should have been be roughly twice that after the ablative exposure. The smaller than expected radical signal in the low laser intensity case has at least three possible causes: (1) statistical variations in the measurement, (2) saturation of the tissue rad-

ical accumulation with repetitive low-intensity irradiation, and (3) a small (factor of ~2) intensity dependence in the quantum efficiency for radical generation.

Assuming the radical quantum yield calculated in this study is close to the value for in vivo corneal ablation, the number of transient free radicals generated in the living tissue is biologically significant. Using the measured 2,700 cm^{-1} small-signal absorption coefficient and 30 mJ/cm^2 ablation threshold fluence, the density of absorbed 193 nm photons near the surface of the unablated corneal tissue is calculated to be $\sim 8 \times 10^{19}$ cm^{-3}. A 0.15% efficiency for radical generation implies that 1.2×10^{17} cm^{-3} of these reactive species are introduced into the tissue surface region with each laser pulse. Given the pronounced biologic impact that free radicals can have, a localized 0.2 mM concentration is quite significant. This finding helps explain the measured reduction in postoperative "haze" by radical scavenger treatment noted earlier [7] and suggests that such pharmacologic therapy may prove useful in modulating the overall corneal healing response.

REFERENCES

1. Trokel SL, Srinivasan R, Braren B. Excimer laser surgery of the cornea. Am J Ophthalmol 1983; 96:710–715.
2. Landry RJ, Pettit GH, Hahn DW, Ediger MN, Yang GC. Preliminary evidence of free radical formation during argon fluoride excimer laser irradiation of corneal tissue. Lasers Light Ophthalmol 1994; 6:87–90.
3. Ediger MN, Pettit GH, Weiblinger RP, Chen CH. Transmission of corneal collagen during ArF excimer laser ablation. Lasers Surg Med 1993; 13:204–210.
4. Del Pero RA, Gigstad JE, Roberts AD, Klintworth GK, Martin CA, L'Esperance FA, Taylor DM. A refractive and histopathologic study of excimer laser keratectomy in primates. Am J Ophthalmol 1990; 109:419–429.
5. Hanna KD, Pouliquen YM, Savoldelli M, Fantes F, Thompson KP, Waring GE, Sams J. Corneal wound healing in monkeys 18 months after excimer laser photorefractive keratectomy. Refract Corneal Surg 1990; 6:340–345.
6. Lohmann CP, Timberlake GT, Fitzke FW, Gartry DS, Kerr Muir M, Marshall J. Corneal light scattering after excimer laser photorefractive keratectomy; the objective measurements of haze. Refract Corneal Surg 1992; 8:114–121.
7. Jain S, Hahn TW, Chen W, Stark W, Chen L, Azar DT. Modulation of corneal wound healing following 193-nm excimer laser keratectomy using free radical scavengers. Invest Ophthalmol Vis Sci 1994; 35:2015.
8. Puliafito CA, Steinert RF, Deutsch TF, Hillenkamp F, Dehm EJ, Adler CM. Excimer laser ablation of the cornea and lens. Ophthalmology 1985; 92:741–748.
9. Glassman I. "Combustion." Orlando: Academic Press, 1987:85–86.
10. Stief LJ, DeCarlo VJ. Vacuum-ultraviolet photochemistry. IX. Primary and chain processes in the photolysis of hydrogen peroxide. J Chem Phys 1969; 50:1234–1240.